

Imaging the hierarchical Ca^{2+} signalling system in HeLa cells

Martin Bootman*, Ernst Niggli†, Michael Berridge* and Peter Lipp*††

† *Department of Physiology, University of Bern, Buehlplatz 5, CH-3012 Bern, Switzerland,*
and * *The Babraham Institute Laboratory of Molecular Signalling, Department of Zoology,*
University of Cambridge, Downing Street, Cambridge CB2 3EJ, UK

1. Confocal microscopy was used to investigate hormone-induced subcellular Ca^{2+} release signals from the endoplasmic reticulum (ER) in a prototype non-excitabile cell line (HeLa cells).
2. Histamine application evoked two types of elementary Ca^{2+} signals: (i) Ca^{2+} blips arising from single ER Ca^{2+} release channels (amplitude, 30 nM; lateral spreading, 1.3 μm); (ii) Ca^{2+} puffs resulting from the concerted activation of several Ca^{2+} blips (amplitude, 170 nM; spreading, 4 μm).
3. Ca^{2+} waves in the HeLa cells arose from a variable number of initiation sites, but for individual cells, the number and subcellular location of the initiation sites were constant. The kinetics and amplitude of global Ca^{2+} signals were directly proportional to the number of initiation sites recruited.
4. Reduction of the feedback inherent in intracellular Ca^{2+} release caused saltatoric Ca^{2+} waves, revealing the two principal steps underlying wave propagation: diffusion and regeneration. Threshold stimulation evoked abortive Ca^{2+} waves, caused by the limited recruitment of Ca^{2+} puffs.
5. The hierarchy of Ca^{2+} signalling events, from fundamental levels (blips) to intermediate levels (puffs) to Ca^{2+} waves, is a prototype for Ca^{2+} signal transduction for non-excitabile cells, and is also analogous to the Ca^{2+} quarks, Ca^{2+} sparks and Ca^{2+} waves in cardiac muscle cells.

Many electrically non-excitabile cells respond to hormonal stimulation with an increase in inositol 1,4,5-trisphosphate (InsP_3) production and a concomitant increase in the cytoplasmic calcium concentration ($[\text{Ca}^{2+}]_i$) (Berridge, 1993; Petersen, Petersen & Kasai, 1994). At the whole-cell level, hormone-induced Ca^{2+} transients are frequently observed as a series of repetitive spikes or oscillations. The subcellular correlate of Ca^{2+} spikes is waves, where $[\text{Ca}^{2+}]_i$ is initially elevated in a localized region and then propagates across the cell in a regenerative manner (Bootman & Berridge, 1996).

Recent evidence has suggested that intracellular Ca^{2+} signals may be generated by the recruitment of functionally discrete intracellular Ca^{2+} release units. These Ca^{2+} release units have been proposed to comprise the elementary building blocks for global Ca^{2+} signals such as spikes and waves (Bootman & Berridge, 1995). Examples of elementary Ca^{2+} release events are the Ca^{2+} puffs in *Xenopus* oocytes (Yao, Choi & Parker, 1995), and the Ca^{2+} sparks in muscle cells (Cheng, Lederer & Cannell, 1993; Lipp & Niggli, 1994; López-López, Shacklock, Balke & Wier, 1995; Nelson *et al.* 1995; Tsugorka, Rios & Blatter, 1995; Klein, Cheng, Santana, Jiang, Lederer &

Schneider, 1996). Although puffs arise from clusters of InsP_3 receptors (InsP_3Rs), whilst sparks represent Ca^{2+} release from clusters of ryanodine receptors (RyRs), these two classes of subcellular events may represent analogous activities.

The seminal work of Parker and colleagues on Ca^{2+} puffs in *Xenopus* oocytes has provided crucial information about the nature of Ca^{2+} release at the microscopic level in these large oocytes. However, it is unclear whether other typical non-excitabile cells have the same functional architecture. Estimates of the size and distribution of Ca^{2+} puffs in *Xenopus* oocytes suggested that cells of a more typical volume might only contain one such release unit (Parker & Yao, 1992). In addition, although it was hypothesized that summation of Ca^{2+} puffs results in global Ca^{2+} transients, there is as yet no direct evidence that wave propagation involves sequential recruitment of elementary Ca^{2+} release events. Furthermore, the Ca^{2+} puffs demonstrated in *Xenopus* oocytes were activated by an exogenous elevation of InsP_3 , following microinjection or photolytic liberation from InsP_3 analogues.

†† To whom correspondence should be addressed at The Babraham Institute, Babraham Hall, Babraham, Cambridge CB2 4AT, UK.

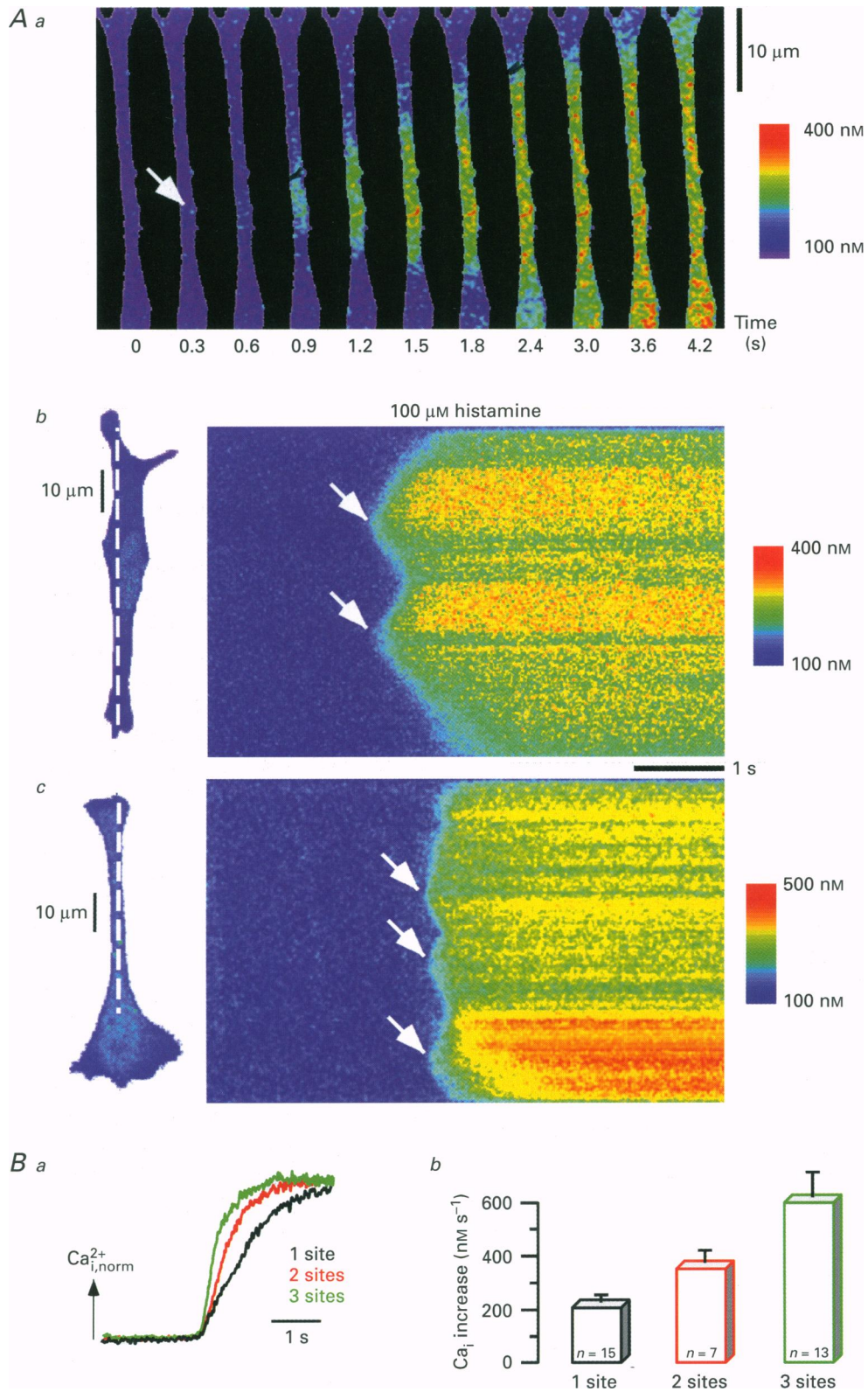


Figure 1. For legend see facing page.

Here, we have used HeLa cells, prototypic non-excitabile cells, to investigate subcellular Ca^{2+} signals following hormonal activation of the phosphoinositide signal transduction cascade. We demonstrate the existence of a hierarchical Ca^{2+} signalling system in the HeLa cells, comprising fundamental Ca^{2+} blips, intermediate Ca^{2+} puffs and global Ca^{2+} waves, and furthermore show the functional interconnection between the different levels of this hierarchy.

METHODS

Calcium measurements

HeLa cell culture and preparation for imaging was performed as described previously (Bootman, Cheek, Moreton, Bennett & Berridge, 1994). The culture medium was replaced with an extracellular medium containing (mM): NaCl, 121; KCl, 5.4; $MgCl_2$, 0.8; $CaCl_2$, 1.8; $NaHCO_3$, 6; glucose, 5.5; Hepes, 25; pH 7.3. Cells were loaded with fluo-3 by incubation with 2 μM fluo-3 acetoxymethyl ester (Molecular Probes) for 30 min, followed by a 30 min de-esterification period. All incubations and experiments were carried out at room temperature (20–22 °C). Confocal cell imaging was performed as described elsewhere (Lipp & Niggli, 1994). Briefly, a single glass coverslip was mounted on the stage of a Nikon Diaphot inverted microscope attached to a BioRad MRC-1000 laser-scanning confocal microscope (BioRad, Glattbrugg, Switzerland), equipped with a standard argon ion laser for illumination. Fluo-3 was excited with the 488 nm laser line, and the emitted fluorescence was collected at wavelengths > 515 nm. Confocal images were acquired either in image or linescan mode. For line scanning, a single line (shown in the cell images as a dashed white line) was chosen from the entire confocal section and repetitively scanned every 12 ms. The successive lines were stacked horizontally to compile an image where time increased from left to right, and the spatial dimension was preserved in the vertical axis. Absolute values for $[Ca^{2+}]_i$ were calculated according to a self-ratio method. All the experiments presented in this study were performed in a Ca^{2+} -containing medium. However, the responses shown represent endoplasmic reticulum (ER) Ca^{2+} release with little contribution from Ca^{2+} entry, since similar observations were made using cells in a Ca^{2+} -free medium (data not shown).

Calculations

The Ca^{2+} flux (J) associated with subcellular Ca^{2+} release signals was calculated using $J = B\Delta[Ca^{2+}]_i V/t_{up}$ (Cheng *et al.* 1993), where B is the Ca^{2+} buffering capacity of the intracellular milieu (ratio of bound Ca^{2+} over free Ca^{2+}), $\Delta[Ca^{2+}]_i$ the Ca^{2+} concentration change during the signal, V the volume occupied by the signal and t_{up} the rise time. B was taken to be 40 (Zhou & Neher, 1993). The volume occupied by the signals was calculated by integration of a Gaussian distribution for three dimensions, assuming a homogeneous spreading of Ca^{2+} ions in all directions.

RESULTS

HeLa cells exhibit variable numbers of Ca^{2+} wave initiation sites

Rapid application of a supramaximal histamine concentration (100 μM) evoked Ca^{2+} waves in the HeLa cells, which originated from a variable number of initiation sites; 70% of the cells had an individual site ($n = 35$; Fig. 1*A a*), and 30% had two (Fig. 1*A b*) or more foci (Fig. 1*A c*). The consequence of the variable number of initiation sites is apparent from the kinetics and amplitude of the Ca^{2+} signal; both the upstroke velocity (Fig. 1*B*) and the magnitude (data not shown) of the Ca^{2+} signals were directly proportional to the number of initiation sites. In the majority of cells, the location of the initiation foci was constant; the same sites initiated Ca^{2+} waves during repetitive histamine applications (data not shown). Since the volume of the cell imaged in the linescan mode is only a fraction ($\sim 1\%$) of the whole cell, the actual number of initiation sites may be higher.

Threshold stimulation evokes abortive Ca^{2+} waves

Previous studies have shown that the amplitude of histamine-stimulated $[Ca^{2+}]_i$ rises in HeLa cells can be graded with the agonist concentration, and that threshold stimulation causes abortive responses which fail to become fully regenerative (Bootman *et al.* 1994). In the present study, global Ca^{2+} waves stimulated by supramaximal histamine concentrations (Figs 1 and 2*A a* upper panel) were reduced to abortive Ca^{2+} signals with limited subcellular propagation by threshold stimulation, as shown in the lower panel of Fig. 2*A*. Since re-application of a supramaximal histamine concentration again induced a global Ca^{2+} wave (data not shown), this abortive Ca^{2+} release was not due to desensitization of the Ca^{2+} releasing machinery. Instead, the time course of the response (Fig. 2*A c* green curve) shows a distinct, quantized Ca^{2+} signal preceding the abortive transient, similar to the Ca^{2+} puffs in *Xenopus* oocytes (Yao *et al.* 1995). These data indicate that application of a weak stimulus to HeLa cells evokes spatially restricted Ca^{2+} release from the ER, and within such responses elementary Ca^{2+} signals (Ca^{2+} puffs) become visible.

Ca^{2+} puffs underlie Ca^{2+} wave initiation

Similar Ca^{2+} puffs were occasionally evident as triggering events for global Ca^{2+} waves evoked by supramaximal stimulation (Fig. 2*B*; 25% of all responses; $n = 40$ cells). The time course of the elementary event is shown in Fig. 2*B c* as the difference between the Ca^{2+} signal in the region of the

Figure 1. Histamine-stimulated Ca^{2+} waves in fluo-3-loaded HeLa cells

A, confocal image sequence (*A a*), or linescan images (*A b* and *A c*) showing the initiation sites of histamine-stimulated Ca^{2+} waves (100 μM histamine). Responses with one (*A a*), two (*A b*) and three (*A c*) initiation sites (marked with white arrows) are displayed. Histamine superfusion began at the start of each recording. *B*, the consequence of the number of initiation events on the kinetics of the histamine-stimulated $[Ca^{2+}]_i$ rise. *B a*, time courses for the Ca^{2+} signals in *A a* (single initiation site; black line), *A b* (two initiation sites; red line) and *A c* (three initiation sites; green line), obtained by averaging across the spatial dimension of the linescan images. Since the amplitude of the Ca^{2+} signals was also directly proportional to the number of initiation sites, the curves were normalized to the response shown by the green line. *B b* illustrates the averaged rate of rise of the Ca^{2+} signals (data are means \pm s.e.m.; number of cells is given in the bars).

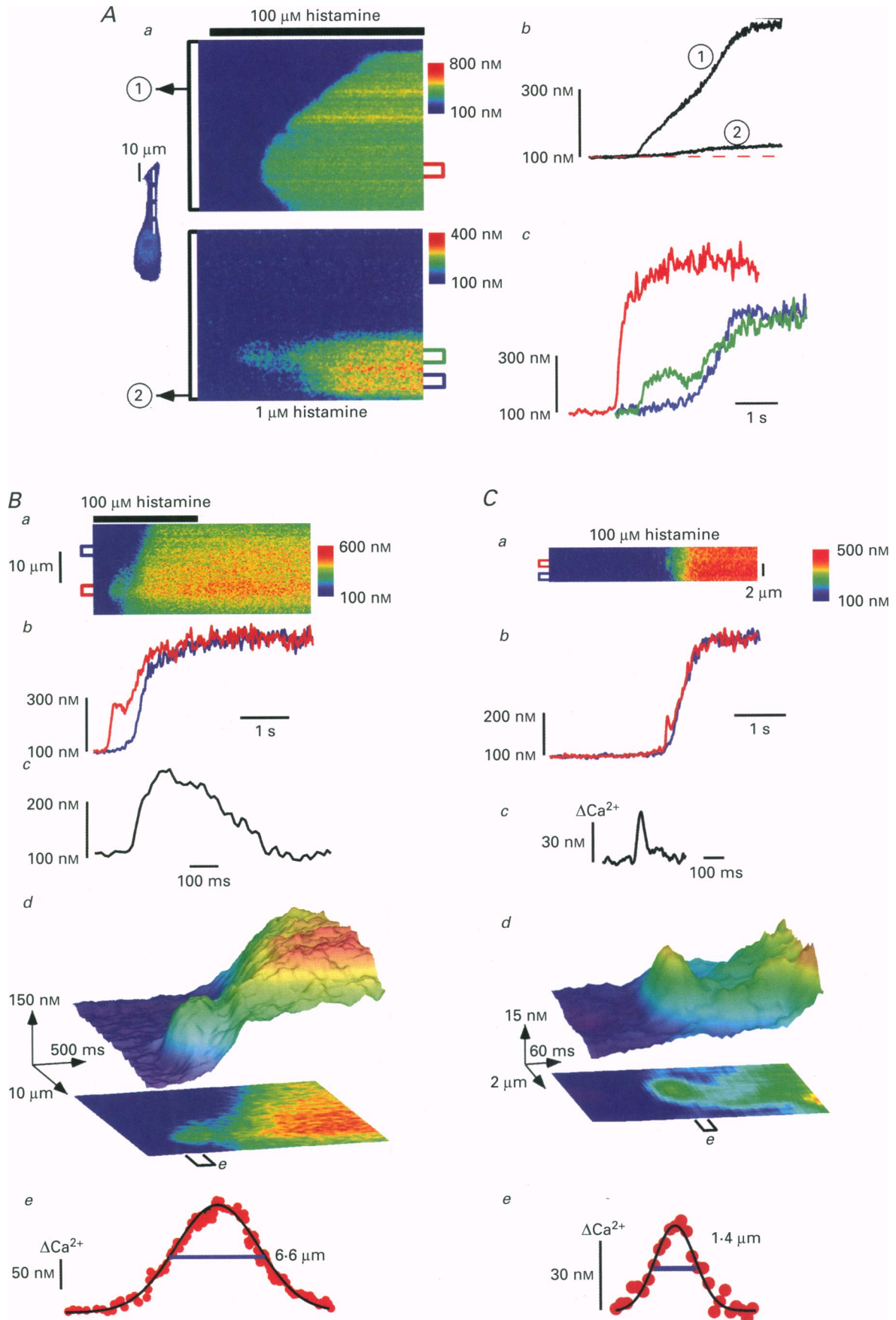


Figure 2. For legend see facing page.

event (red curve in Fig. 2*Bb*) and an adjacent area (blue curve in Fig. 2*Bb*). While global Ca^{2+} waves take a few seconds for propagation in HeLa cells, these elementary signals were brief events ($t_{1/2}$ for upstroke, ~ 42 ms; $t_{1/2}$ for relaxation, ~ 180 ms), with limited subcellular spreading ($4\text{--}7\ \mu\text{m}$; Figs 2*Bd* and *e*). Although a temporal separation between the initiation signal and the propagating Ca^{2+} wave was not always evident (e.g. Figs 1*B* and 2*A* upper panel), we suggest that Ca^{2+} puffs underlie Ca^{2+} wave initiation in HeLa cells.

Imaging of fundamental Ca^{2+} blips

In addition to Ca^{2+} puffs, which are the intermediate elementary Ca^{2+} signals in HeLa cells, Fig. 2*C* presents evidence for the existence of smaller fundamental Ca^{2+} release events. In five different cells, brief ($t_{1/2}$ for upstroke, ~ 12 ms; $t_{1/2}$ for relaxation, ~ 45 ms) and highly confined (spreading, $\sim 1.3\ \mu\text{m}$) Ca^{2+} signals (amplitude, ~ 30 nM) were observed preceding cellular Ca^{2+} transients (Fig. 2*Ca*). The temporal (Fig. 2*Cb* and *c*) and spatial (Fig. 2*Cd* and *e*) properties of one such event are illustrated. The Ca^{2+} flux associated with these 'Ca²⁺ blips' was calculated (see Methods) to be 3×10^{-18} mol s^{-1} , corresponding to an ionic current of ~ 1 pA. Similar calculations performed for the HeLa cell Ca^{2+} puffs indicated a larger Ca^{2+} flux (7×10^{-17} mol s^{-1} ; ~ 25 pA).

Spatiotemporal recruitment of Ca^{2+} puffs: saltatoric waves

Current models for hormone-evoked Ca^{2+} wave propagation are based on a Ca^{2+} -induced Ca^{2+} release (CICR) mechanism, where sequential activation of Ca^{2+} release sites is triggered by diffusion of Ca^{2+} between these sites. However, the nature of the event(s) at the release sites has not been fully elucidated. In native HeLa cells, histamine evoked smoothly spreading Ca^{2+} waves, e.g. Fig. 1. This continuous wave propagation results from high positive feedback in the CICR mechanism, while abortive Ca^{2+} waves, e.g. Fig. 2*A*, are due to low positive feedback. An intermediate level of positive feedback would allow the Ca^{2+} wave to propagate in a saltatoric manner, as displayed in Fig. 3*A*. This discontinuous propagation clearly shows the principal steps of regeneration

and diffusion that underlie Ca^{2+} wave propagation. In addition, from the dimensions of the regenerative sites, we suggest that the underlying elements are most likely Ca^{2+} puffs. This saltatoric wave displayed five peaks in the propagation velocity over the $38\ \mu\text{m}$ distance analysed (Fig. 3*B*), giving an average Ca^{2+} puff spacing of $\sim 7.6\ \mu\text{m}$.

Spatiotemporal recruitment of Ca^{2+} blips: microscopic Ca^{2+} wave within a Ca^{2+} puff

Unlike the Ca^{2+} puffs in Fig. 2*A* and *B*, the puff which initiated the saltatoric Ca^{2+} wave in Fig. 3 was not symmetrical around its point of origin, as shown in the enlarged representation in Fig. 3*C* (contrast the initiation of the Ca^{2+} puff denoted *a* with the much more homogeneous Ca^{2+} puff denoted *b*). Instead, this response was preceded by a smaller Ca_i^{2+} signal, possibly a Ca^{2+} blip, that was near the lower edge of the puff site (Fig. 3*Ca*). This small initiation event triggered a Ca^{2+} wave within the Ca^{2+} puff site. This transition of Ca^{2+} signals from blips to puffs to waves, demonstrates the entire hierarchy of intracellular Ca^{2+} signals at a single locus within a HeLa cell.

DISCUSSION

In the present study, we demonstrated the hierarchical Ca^{2+} signalling system in HeLa cells, and that different levels of the hierarchy are linked by the spatiotemporal recruitment of elementary events. In addition, we visualized the coexistence of multiple Ca^{2+} puff sites in an individual HeLa cell (Figs 1 and 3), responsible for both Ca^{2+} wave initiation and propagation (Figs 2 and 3).

The fundamental events of the hierarchy, Ca^{2+} blips, can be observed in isolation (Fig. 2*C*), can trigger Ca^{2+} puffs (Fig. 3*C*) or can summate in a stepwise manner (Fig. 4*Aa* and 4*B*) and initiate Ca^{2+} waves. The intermediate events, Ca^{2+} puffs, represent the major Ca^{2+} wave initiation signal (Figs 2, 4*Ab* and 4*B*), and furthermore are the events underlying wave propagation, as evident from saltatoric Ca^{2+} waves (Fig. 3). The blips and puffs described in the present

Figure 2. Fundamental and intermediate elementary Ca^{2+} signals in HeLa cells

A, comparison of Ca^{2+} signals evoked by supramaximal (*Aa* upper panel) and threshold stimulation (*Aa* lower panel) of a HeLa cell with histamine. Due to different latencies for the responses, $100\ \mu\text{M}$ histamine was added as shown by the filled bar, and $1\ \mu\text{M}$ histamine was added 5 s prior to starting the linescan. $[\text{Ca}^{2+}]_i$ averaged from the linescans in *Aa* is replotted in *Ab*. The curves labelled 1 and 2 correspond to $[\text{Ca}^{2+}]_i$ averaged across the entire spatial dimension for the 100 and $1\ \mu\text{M}$ responses, respectively. The red, green and blue traces in *Ac* were obtained from the corresponding coloured regions marked in *Aa*. The green trace shows a Ca^{2+} puff preceding an abortive Ca^{2+} wave. *Ba*, a Ca^{2+} puff at the initiation site of a Ca^{2+} wave. The time course of the $[\text{Ca}^{2+}]_i$ rise is shown in *Bb*, for both a region including the Ca^{2+} puff (red curve) and an adjacent area without a puff (blue curve). Subtraction of the red and blue lines in *Bb* gave the time course of the Ca^{2+} puff is shown in *Bc*. The Ca^{2+} puff is replotted in *Bd* as a surface representation with the corresponding part of the linescan taken from *Ba*. $[\text{Ca}^{2+}]_i$ is coded in both the height and colour of the surface. The spatial spreading of the Ca^{2+} puff is shown in *Be*. The continuous line in *Be* was obtained by a Gaussian fitted to the points. *Ca*, a linescan from a histamine-stimulated HeLa cell displaying a Ca^{2+} blip before the onset of the global signal. The red and blue lines in *Cb* represent the averaged $[\text{Ca}^{2+}]_i$ from the corresponding coloured regions marked in *Ca*. The time course of the Ca^{2+} blip shown in *Cc*, was obtained by subtracting the blue line from the red. *Cd* shows a surface representation of the Ca^{2+} blip with part of the linescan from *Ca*. The spatial spreading of the Ca^{2+} blip is shown in *Ce*.

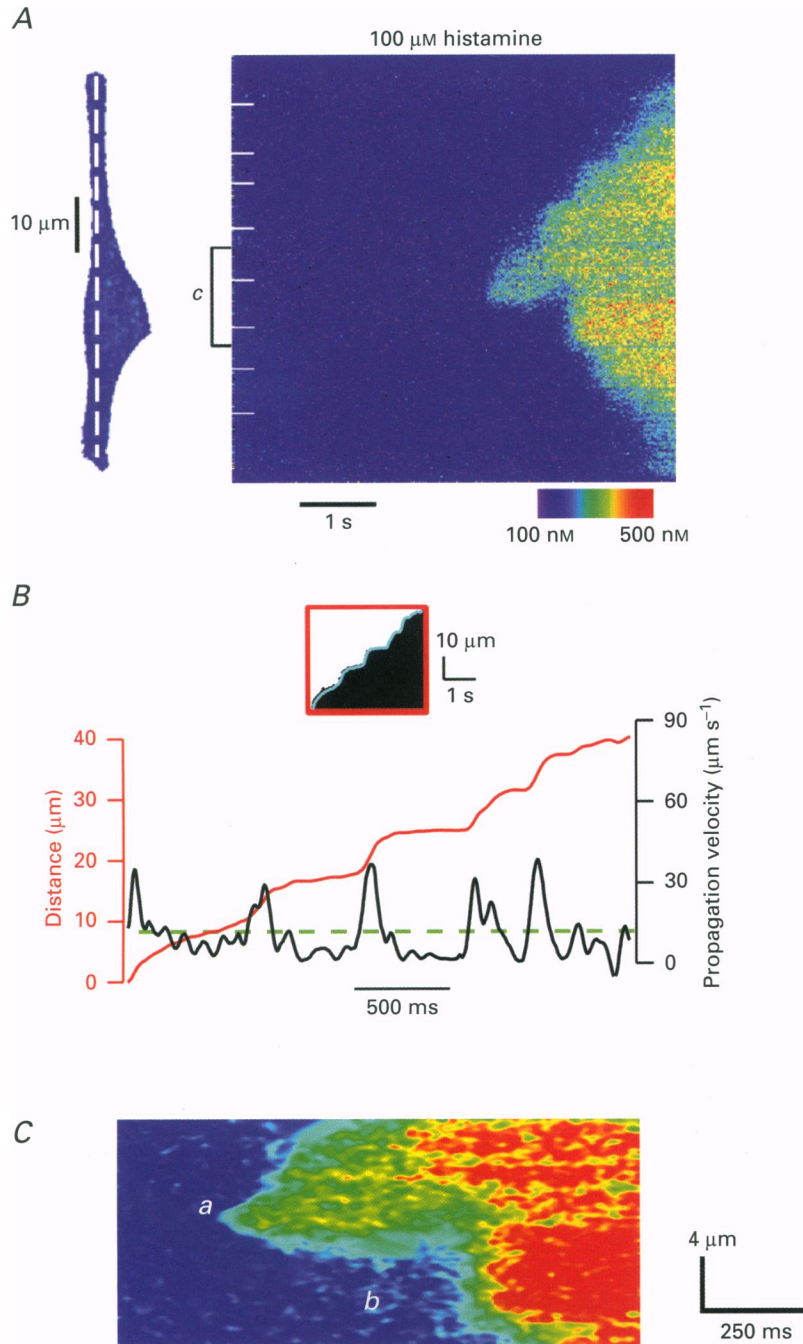


Figure 3. Saltatoric Ca^{2+} wave propagation

The linescan in *A* shows the third response of a cell to repeated 5 s applications of histamine interspersed by 3 min resting periods. Since repetitive histamine stimulation often causes the amplitude of the Ca^{2+} signal to decline and the latency of the Ca^{2+} signal to increase, this linescan image represents a partially desensitized response. For each histamine stimulation, the Ca^{2+} waves initiated at the same site. However, in contrast to the waves stimulated by the first two histamine applications, which showed a continuous propagation profile, the third response resulted in a discontinuous wave propagation. This behaviour was observed in 3 different cells. Putative Ca^{2+} puff sites are marked by the white lines on the left side of the linescan image. The saltatory changes of the propagation velocity during the Ca^{2+} wave are plotted in *B*. In order to calculate the position of the wave front with time, the linescan image from *A* was transformed into a black–white contrast image (inset in *B*) by thresholding at a $[\text{Ca}^{2+}]_i$ of 200 nM. The wavefront in this black–white representation was calculated by finding the edges (blue line in inset and red line in main figure). The red curve in *B* therefore shows the propagating front of the saltatory wave at 200 nM amplitude. Velocity of propagation (black curve) was obtained by differentiating this curve with respect to time, and can be seen to consist of peaks and troughs. Peak propagation velocity approached nearly $40 \mu\text{m s}^{-1}$, while the average velocity of the saltatory Ca^{2+} wave (dashed green curve) was $10 \mu\text{m s}^{-1}$. *C*, comparison of the initiating Ca^{2+} puff (marked *a*) and a subsequent puff (marked *b*) during saltatory propagation. The initiating Ca^{2+} puff was characterized by a shallow rising phase with an obvious propagation of the Ca^{2+} signal within the puff site.

Figure 4. The hierarchical Ca^{2+} signalling system in non-excitabile cells

A, recruitment and summation links the different levels of Ca^{2+} signalling in HeLa cells. The blue and red traces in *A a* and *A b*, respectively, illustrate original data obtained from histamine-stimulated HeLa cells. On the right-hand side of the traces are models proposing a sequence of microscopic events leading to subcellular and global Ca^{2+} signals. For each sequence, time runs from bottom to top, and the arrows connect each panel with a corresponding time point on the original Ca^{2+} record. Each original tracing was averaged from a $2 \mu\text{m}$ wide band across a linescan image, and is representative of 10 linescan images from 5 different cells. *A a*, recruitment of individual Ca^{2+} blips from of a cluster of InsP_3Rs (a cluster is arbitrarily given five InsP_3Rs). *A b*, recruitment of a Ca^{2+} puff via concerted activity of the entire cluster of InsP_3Rs . Horizontal scale bars, 150 ms; vertical scale bars, $150 \mu\text{m}$. *B*, schematic representation of the hierarchy of intracellular Ca^{2+} signals. In order to visualize the spatiotemporal linkage of subcellular Ca^{2+} signals, this model is a pseudo-linescan representation with time running from left to right. The lower (black) path indicates that blips occur from the opening of single InsP_3Rs within clusters. Puffs (middle, red path) occur via the co-ordinated opening of multiple InsP_3Rs within each cluster. Both blips and puffs can initiate global Ca^{2+} signals via a recruitment process (blue and red paths).

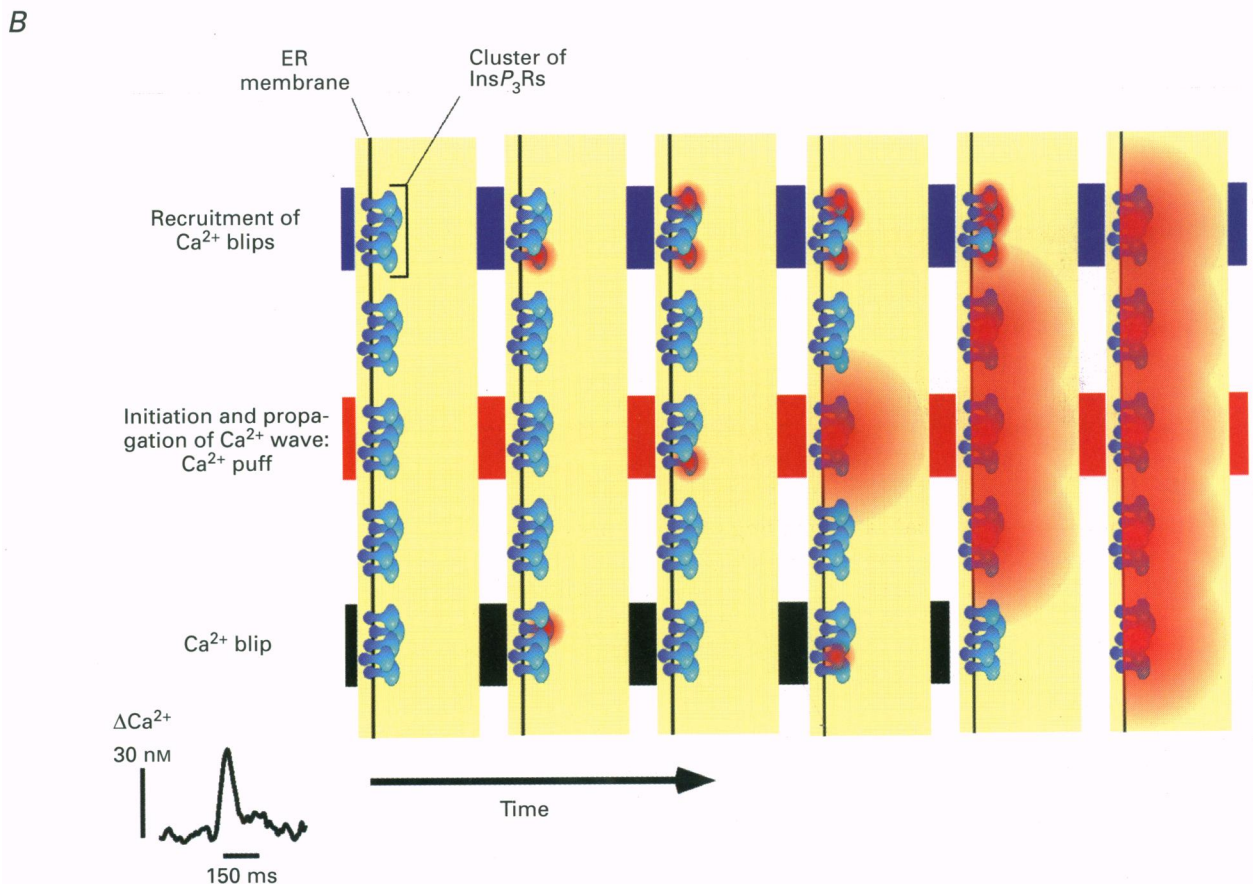
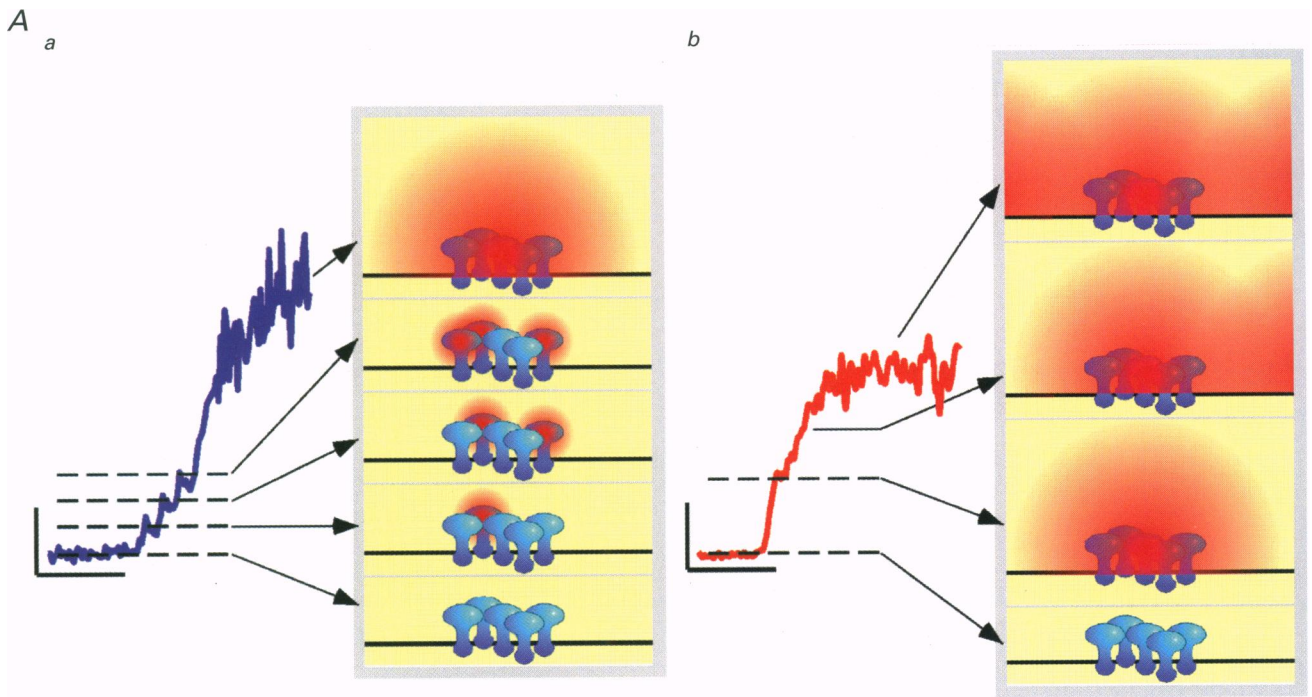


Figure 4. For legend see facing page.

study were the only types of elementary Ca^{2+} signals observed in the HeLa cells.

The calculated ionic current associated with blips (~ 1 pA) is consistent with the conductance of a single InsP_3R (Bezprozvanny & Erlich, 1995; Stehno-Bittel, Luckhoff & Clapham, 1995), compatible with these events arising from the gating of individual InsP_3Rs , as hypothesized for *Xenopus* oocyte Ca^{2+} blips (Parker & Yao, 1996). In this case, the 25-fold larger puffs would represent the opening of multiple InsP_3Rs . Further evidence that puffs result from multiple InsP_3Rs is the propagation of a Ca^{2+} wave within a puff site (e.g. Fig. 3C). This microscopic Ca^{2+} wave within a Ca^{2+} puff is consistent with a spatiotemporal recruitment of InsP_3Rs probably via CICR, and is therefore a microscopic analogue of the propagation of global Ca^{2+} waves.

Summation of Ca^{2+} release from a differential number of Ca^{2+} puff sites within cells (Fig. 1) may underlie the intercellular variation in kinetics and amplitude of Ca_i^{2+} signals. In addition, the concentration-dependent recruitment of Ca^{2+} puff sites within a cell may underlie the graded or 'quantal' responses that are apparent in HeLa (Fig. 2A) and other intact cells (Bootman *et al.* 1994). One scheme proposed to explain such responses suggests that $[\text{Ca}^{2+}]_i$ is graded due to the stimulus-dependent release of functionally independent Ca^{2+} stores, which individually contribute a quantized amount of Ca^{2+} (Parys, Missiaen, De Smedt, Sienaert & Casteels, 1996). The spatially restricted response to $1 \mu\text{M}$ histamine supports the notion of functional compartmentation of the ER.

The hierarchy of Ca^{2+} signals described in this study, from blips to puffs to waves, not only applies to non-excitabile cells, such as *Xenopus* oocytes or HeLa cells, but is also applicable to excitable cells, such as cardiac myocytes (Niggli & Lipp, 1995; Lipp & Niggli, 1996). In these cells, the gating of single RyRs may evoke Ca^{2+} quarks, which represent the fundamental level of signalling analogous to blips. Simultaneous activation of a cluster of RyRs gives rise to Ca^{2+} sparks, reflecting the intermediate elementary events analogous to puffs. On the next level of Ca^{2+} signalling, spatial and temporal recruitment of Ca^{2+} sparks gives rise to global transients, i.e. Ca^{2+} waves and homogeneous Ca^{2+} transients. Thus, the concept of a hierarchy of intracellular Ca^{2+} signals, and linkage of the different levels, may therefore be generally applicable to signal transduction processes utilizing Ca^{2+} .

BERRIDGE, M. J. (1993). Inositol trisphosphate and calcium signalling. *Nature* **361**, 315–325.

BEZPROZVANNY, I. & EHRLICH, B. E. (1995). The inositol 1,4,5-trisphosphate (InsP_3) receptor. *Journal of Membrane Biology* **145**, 205–216.

BOOTMAN, M. D., CHEEK, T. R., MORETON, R. B., BENNETT, D. L. & BERRIDGE, M. J. (1994). Smoothly graded Ca^{2+} release from inositol 1,4,5-trisphosphate-sensitive Ca^{2+} stores. *Journal of Biological Chemistry* **269**, 24783–24791.

BOOTMAN, M. D. & BERRIDGE, M. J. (1995). The elemental principles of calcium signalling. *Cell* **83**, 675–678.

BOOTMAN, M. D. & BERRIDGE, M. J. (1996). Subcellular Ca^{2+} signals underlying waves and graded responses in HeLa cells. *Current Biology* **6**, 855–865.

CHENG, H., LEDERER, W. J. & CANNELL, M. B. (1993). Calcium sparks – elementary events underlying excitation-contraction coupling in heart muscle. *Science* **262**, 740–744.

KLEIN, M. G., CHENG, H., SANTANA, L. F., JIANG, Y.-H., LEDERER, W. J. & SCHNEIDER, M. F. (1996). Two mechanisms of quantized calcium release in skeletal muscle. *Nature* **379**, 455–458.

LIPP, P. & NIGGLI, E. (1994). Modulation of Ca^{2+} release in cultured neonatal rat cardiac myocytes – insight from subcellular release patterns revealed by confocal microscopy. *Circulation Research* **74**, 979–990.

LIPP, P. & NIGGLI, E. (1996). Submicroscopic calcium signals as fundamental events of excitation-contraction coupling in guinea-pig cardiac myocytes. *Journal of Physiology* **492**, 31–38.

LÓPEZ-LÓPEZ, J. R., SHACKLOCK, P. S., BALKE, C. W. & WIER, W. G. (1995). Local calcium transients triggered by single L-type calcium channel currents in cardiac cells. *Science* **268**, 1042–1045.

NELSON, M. T., CHENG, H., RUBART, M., SANTANA, L. F., BONEV, A. D., KNOT, H. J. & LEDERER, W. J. (1995). Relaxation of arterial smooth muscle by calcium sparks. *Science* **270**, 633–637.

NIGGLI, E. & LIPP, P. (1995). Subcellular features of calcium signalling in heart muscle – what do we learn? *Cardiovascular Research* **29**, 441–448.

PARKER, I. & YAO, Y. (1992). Regenerative release of calcium from functionally discrete subcellular stores by inositol trisphosphate. *Proceedings of the Royal Society B* **246**, 269–274.

PARKER, I. & YAO, Y. (1996). Ca^{2+} transients associated with openings of inositol trisphosphate-gated channels in *Xenopus* oocytes. *Journal of Physiology* **491**, 663–668.

PARYS, J. B., MISSIAEN, L., DE SMEDT, H., SIENAERT, I. & CASTEELS, R. (1996). Mechanisms responsible for quantal Ca^{2+} release from inositol trisphosphate-sensitive calcium stores. *Pflügers Archiv* **432**, 359–367.

PETERSEN, O. H., PETERSEN, C. C. H. & KASAI, H. (1994). Calcium and hormone action. *Annual Review of Physiology* **56**, 297–319.

STEHNO-BITTEL, L., LUCKHOFF, A. & CLAPHAM, D. E. (1995). Calcium release from the nucleus by InsP_3 receptor channels. *Neuron* **14**, 163–167.

TSUGORKA, A., RIOS, E. & BLATTER, L. A. (1995). Imaging the elementary aspects of calcium release in skeletal muscle. *Science* **269**, 1723–1726.

YAO, Y., CHOI, J. & PARKER, I. (1995). Quantal puffs of intracellular Ca^{2+} evoked by inositol trisphosphate in *Xenopus* oocytes. *Journal of Physiology* **482**, 533–553.

ZHOU, Z. & NEHER, E. (1993). Mobile and immobile calcium buffers in bovine adrenal chromaffin cells. *Journal of Physiology* **469**, 245–273.

Acknowledgements

M.D.B. is a Royal Society University Research Fellow. E.N. was supported by the Swiss National Science Foundation.

Author's email address

P. Lipp: PETER.LIPP@BBSRC.AC.UK

Received 11 December 1996; accepted 8 January 1997.